Journal of Alloys and Compounds 506 (2010) 70–72

Contents lists available at ScienceDirect

Journal of Alloys and Compounds

journal homepage: www.elsevier.com/locate/jallcom

Anisotropic properties and crystal structure of ferroelectric $Na_{0.5}Bi_{4.5}Ti_4O_{15}$

Zhengfa Li[a,b,c,*], H.L.W. Chan[a], Yongxiang Li[b,*], K.W. Kwok[a], S.H. Choy[a]

[a] Department of Applied Physics & Materials Research Centre, The Hong Kong Polytechnic University, Kowloon, Hong Kong, PR China
[b] Shanghai Institute of Ceramics & Graduate University of the Chinese Academy of Sciences, Shanghai 200050, PR China
[c] College of Materials Science and Engineering, China Jiliang University, Hangzhou 310018, PR China

ARTICLE INFO

Article history:
Received 19 April 2010
Received in revised form 15 June 2010
Accepted 5 July 2010
Available online 15 July 2010

PACS:
77.22.Ch
77.84.Dy
77.80.Bh
61.10.Nz

Keywords:
Dielectric property
Ferroelectric
$Na_{0.5}Bi_{4.5}Ti_4O_{15}$
Phase transition

ABSTRACT

Bismuth layer-structured ferroelectric sodium bismuth titanate $Na_{0.5}Bi_{4.5}Ti_4O_{15}$ (NBT4) was prepared by conventional solid-state reaction method, and its dielectric and ferroelectric properties are investigated. The dielectric spectra of NBT4 ceramics obviously display anisotropic behaviors, in which the large thermal hysteresis loops with anisotropy are found for first-order phase transitions of NBT4. Based on the analyses of obtained XRD and SEM results, the special anisotropic responses maybe contributed to pseudo-perovskite blocks and bismuth layers $(Bi_2O_2)^{2+}$ for their stages of lattice transitions in NBT4 compound.

1. Introduction

Recently, grain-textured technologies based on nanostructures or special crystal growths have been widely utilized in ferroelectric polymers [1] and ceramics [2]. With the miniaturization tendency of integrated electronic devices, such as ferroelectric random access memories (FRAM), ferroelectric ceramic grains themselves deserve more attention, just as tremendous ones on their ordered assemblies, because of the various anisotropies on properties in single ferroelectric grain along different crystal directions. Particularly are the Aurivillius family materials, bismuth layer-structured ferroelectric (BLSF) ceramics, in which sodium bismuth titanate ($Na_{0.5}Bi_{4.5}Ti_4O_{15}$, NBT4) [3,4] and bismuth titanate ($Bi_4Ti_3O_{12}$, BT) [5–8] ceramics are their representatives. The crystal structure of BLSF materials is expressed commonly as a general formula $(Bi_2O_2)^{2+}(A_{m-1}B_mO_{3m+1})^{2-}$, in which A is a mono- to tri-valent ion and/or combination of cations allowing dodecahedral coordination, B is transition element (Ti^{4+}, Nb^{5+}, Ta^{5+}, W^{6+}) and/or their combination, and the integral m of 1–5 represents the number of BO_6 octahedra in $(A_{m-1}B_mO_{3m+1})^{2-}$ pseudo-perovskite blocks between $(Bi_2O_2)^{2+}$ layers.

As the promising lead-free piezoelectric materials in application at high temperature, four-layered compound NBT4 begins to attract more attention. Some relative high piezoelectric properties have been achieved by changing chemical compositions [9–13] and/or textured microstructure by hot-forging method [14]. Even though the piezoelectric properties of NBT4 were improved dramatically, the mechanism between electrical properties and phase transitions of NBT4 has remained still unclear. Two pressure-induced phase transitions [15] and one temperature-induced phase transition [16] have been observed, respectively. Further studies in-depth on the electrical properties and crystal structures of NBT4 grains under high pressure, external electric field, and different temperatures are needed. In this paper, we report the experimental results of the anisotropic characters of dielectric and ferroelectric properties for conventionally sintered NBT4 ceramics, which maybe derive from pseudo-perovskite blocks and $(Bi_2O_2)^{2+}$ layer in the crystal unit.

2. Experimental

NBT4 ceramic specimens were prepared using a conventional solid-state processing. The starting raw materials were high purity Na_2CO_3 (99.8%), Bi_2O_3 (99%) and TiO_2 (99%). The materials were weighed individually according to the chemical composition of $Na_{0.5}Bi_{4.5}Ti_4O_{15}$, mixed using ball milling, dried and calcined at 850 °C for 3 h. After calcination, the ball-milled ground powders were pressed into disks

* Corresponding authors at: Shanghai Institute of Ceramics, Chinese Academy of Sciences, Shanghai 200050, PR China. Tel.: +86 21 52411066; fax: +86 21 52413122.
E-mail addresses: lizhengfa@cjlu.edu.cn (Z. Li), yxli@mail.sic.ac.cn (Y. Li).

0925-8388/$ – see front matter.
doi:10.1016/j.jallcom.2010.07.022

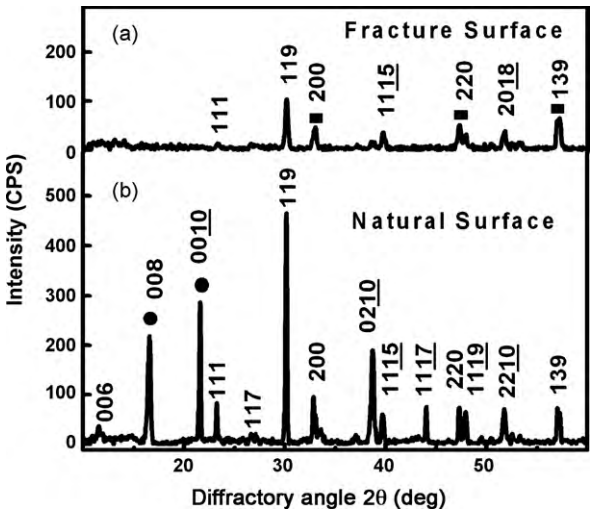

Fig. 1. (a and b) XRD patterns of NBT4 fracture surface perpendicular to radius direction and natural surface.

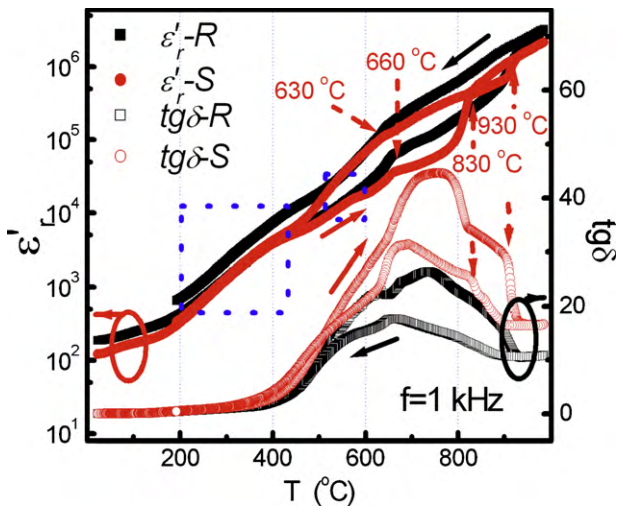

Fig. 3. Temperature dependences of real permittivity (ε'_r) and dielectric loss ($tg\delta$) for NBT4 ferroelectric ceramics.

13 mm in diameter under 200 MPa pressure. Densification was achieved by sintering the disks at 1040 °C for 3 h in a sealed crucible to prevent volatilization. Microstructure characterization of the sintered ceramics was conducted by scanning electron microscopy (SEM, JSM-6490F, JEOL). X-ray diffraction (XRD) patterns for ceramic specimens were obtained with a Philips X'pert XRD System using Cu Kα radiation. The relative permittivity ε'_r and loss tan δ were measured as functions of temperature using an impedance analyzer (HP 4284A). A conventional Sawyer–Tower circuit was used to measure the polarization versus electric field hysteresis (P–E) loop at room temperature and 100 Hz.

3. Results and discussion

Fig. 1 shows the XRD patterns of NBT4 ceramics along fracture surface perpendicular to radius (Fig. 1a) and natural surface (Fig. 1b). It can be seen that NBT4 ceramics are pure compound of Aurivillius phase by contrasting with the literature [16]. Comparing the XRD pattern of NBT4 fracture surface perpendicular to radius (Fig. 1a) with that of natural surface (Fig. 1b), grain orientation along natural surface can be detected obviously by stronger peaks 2θ below 30°, indicating that bismuth layers of most NBT4 grains are more parallel to natural surface than perpendicular to it. Moreover, the intensities of all peaks in Fig. 1a are lower than those in Fig. 1b in the same measuring conditions, implying that bismuth layers maybe have strong effect to weaken X-ray diffraction. Peaks locating around low diffraction angle 2θ of 20° in Fig. 1b cannot be observed in Fig. 1a, showing that texture effect maybe exists widely in the ceramics of Aurivillius family rather than their absolutely random orientation. Correspondingly, diffractive peaks of pseudo-perovskite blocks without the covering of bismuth layers, indicated by black squares (■) in Fig. 1a, can be formed more easily than those in Fig. 1b. The main peaks of (1 1 9) in Fig. 1 remain nearly at the same angle with peak (1 1 7) of ordinarily sintered BT ceramics [6], just with a dispersion of 0.02° between 30.14° in Fig. 1a and 30.16° in Fig. 1b representing the existence of strains in planes (1 1 9) parallel and perpendicular to bismuth layers direction.

The anisotropies of NBT4 grain growth are observed directly from SEM micrographs of fracture surface and natural surface, as shown in Fig. 2 a and b, respectively. NBT4 grains exhibit large plate-like planes with a diameter of around 10 μm and thickness of about 1 μm. Consistently with XRD results, they grew up in the textured formation preferred parallel to ceramic surface rather than perpendicular to it. These provide necessary conditions to investigate the anisotropic electrical properties of NBT4 ceramics along different directions.

The temperature dependences of real permittivity (ε'_r) and dielectric loss ($tg\delta$) at 1 kHz for NBT4 ferroelectrics are shown in Fig. 3, with exponential format to display the changes of dielectric constants sufficiently. The abbreviations of ε'_r -S and ε'_r -R, $tg\delta$-S and $tg\delta$-R represent real permittivities, losses measured perpendicular to the natural surface and along radius direction of NBT4 specimens, respectively. At room temperature, ε'_r -S and ε'_r -R, $tg\delta$-S and $tg\delta$-R are 121.89 and 187.57, 0.0286 and 0.0271, respectively. A large thermal hysteresis loop is detected around the Curie temperature (T_c) [10] of 660 °C, and a small loop is in the range of 830–930 °C for ε'_r -S spectrum, contrarily, only one continuous loop for ε'_r -R displays in the range of 200–930 °C. The phase transitions

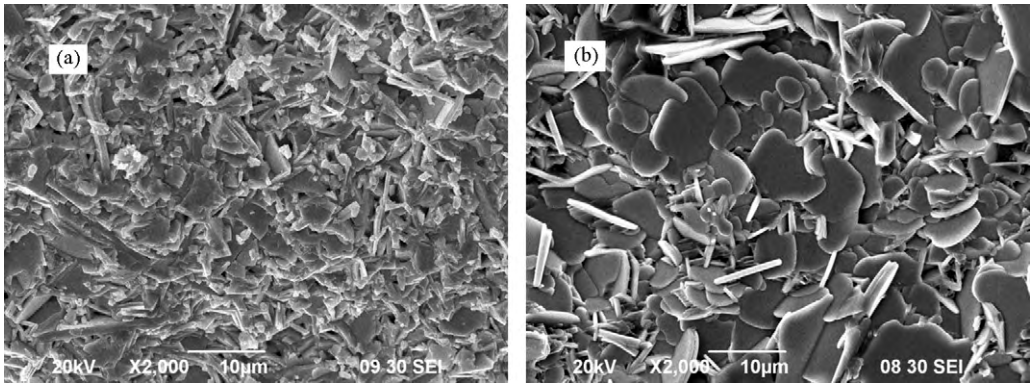

Fig. 2. (a and b) SEM images of the grains on the fracture surface and natural surface of NBT4 ceramics.

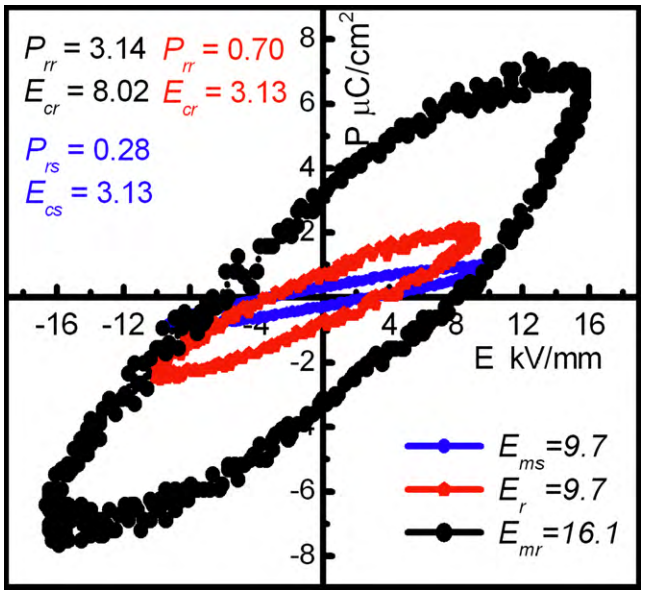

Fig. 4. *P–E* hysteresis loops of NBT4 ceramics measured perpendicular to natural surface and along radius.

of NBT4 are probably first-order ones as thermal hysteresis loop is the well-known character [17]. By the dielectric peaks at 660 °C and 630 °C with increasing and decreasing temperatures, the diffuse phase transition of NBT4 is characterized, and proved by similar peaks of dielectric loss. The distinct diversity between the complex curves of ε_r' -S and ε_r' -R may be interpreted as follows. The crystal structure of chemical formula $Na_{0.5}Bi_{4.5}Ti_4O_{15}$ can be expressed as one perovskite block $Na_{0.5}Bi_{0.5}TiO_3$ (NBT) inserted hypothetically between two bismuth layers of BT. With three pseudo-perovskite blocks $Bi_{2/3}\square_{1/3}TiO_3$ (B□T, where □ denotes cation vacancy) of BT [18], two types of pseudo-perovskite blocks are formed in NBT4 lattice. With the proposed mechanism of layer-by-layer intercalation by defects sweeping across grain [8], the transformation from BT to NBT4 has been verified by at the temperature exceeding 800 °C. A complex sequence of phase transitions of two type perovskite blocks may be traced in Fig. 3, e.g. for the dotted square regions to the thermal hysteresis loop above 200 °C and phase transition above 500 °C are attributed to NBT-liked perovskite blocks [19,20], the dielectric peak at 660 °C to similar BT-liked blocks [6], and a peak at 830 °C to the unification of their cubic lattice parameters with increasing temperature. Finally, the lattice parameters of pseudo-perovskite blocks and bismuth layers maybe fit at about 930 °C, for the superposition of ε_r' above that temperature. Consistently with XRD results in Fig. 1a, all of them are exhibited clearly in ε_r' -R curve without the covering of bismuth layers. It is evident that bismuth layers can shield the thermal hysteresis loop of NBT block, implying that their electrical conductivities are higher than those of pseudo-perovskite blocks in NBT4.

At room temperature, the *P–E* hysteresis loops of NBT4 ceramics are measured perpendicular to natural surface and along radius directions, as shown in Fig. 4. Unlike quasi square-shaped saturated hysteresis loop of NBT [19], NBT4 ceramics show rugby-liked loops for measurements perpendicular to natural surface and along radius. Hence, the spontaneous polarization of pseudo-perovskite blocks maybe are depressed by bismuth layers, especially for applied low electric field. But they possess a larger coercive electric field of 8.02 kV/mm and limiting field intensity of 16.1 kV/mm parallel to natural surface than those of 3.13 kV/mm and 9.7 kV/mm perpendicular to it, and have the similar results of remanent polarizations under a electric field of 9.7 kV/mm. The measured hysteresis loops maybe due to the contributions of pseudo-perovskite blocks and bismuth layers co-existing in NBT4.

4. Conclusions

Summarily, the dielectric and ferroelectric properties of pure NBT4 compound were investigated in this work. Typical NBT-liked and B□T-liked pseudo-perovskite blocks, bismuth layers maybe play their roles in electrical properties and crystal structure, for their preferred orientation in XRD clearly effecting the total performance of NBT4 ceramics. Particularly, the thermal hysteresis loops reveal the stages of diffuse phase transition and the further differences of transformation energy of NBT-liked or B□T-liked blocks.

Acknowledgements

This research was supported by the National High Technology Research and Development Program for Advanced Materials of China (863-Project grant no. 2006AA03Z0433), the State Key Development Program for Basic Research of China (973-Project grant no. 2009CB613305), the Major Program of the National Natural Science Foundation of China (grant no. 50932007) and the Niche Area Projects (grant no. 1-BB95).

References

[1] Z.J. Hu, M.W. Tian, B. Nysten, A.M. Jonas, Nat. Mater. 8 (2009) 62.
[2] Y. Saito, H. Takao, T. Tani, T. Nonoyama, K. Takatori, T. Homma, T. Nagaya, M. Nakamura, Nature 432 (2004) 84.
[3] R.E. Newnham, Mater. Res. Bull. 2 (1967) 1041.
[4] S. Ikegami, I. Ueda, Jpn. J. Appl. Phys. 13 (1974) 1572.
[5] B. Aurivillius, Arkiv. Keni. 1 (1949) 499.
[6] T. Takenaka, K. Sakata, Jpn. J. Appl. Phys. 19 (1980) 31.
[7] T. Watanabe, H. Funakubo, K. Saito, T. Suzuki, M. Fujimoto, M. Osada, Y. Noguchi, M. Miyayama, Appl. Phys. Lett. 81 (2002) 1660.
[8] S. Mallick, K.J. Bowman, A.H. King, Appl. Phys. Lett. 86 (2005) 182902.
[9] C.M. Wang, L. Zhao, J.F. Wang, S.J. Zhang, T.R. Shrout, Phys. Status Solidi: R 3 (2009) 7.
[10] L. Zhao, J.X. Xu, N. Yin, H.C. Wang, C.J. Zhang, J.F. Wang, Phys. Status Solidi: R 2 (2008) 111.
[11] Z.G. Gai, J.F. Wang, M.L. Zhao, W.B. Sun, S.Q. Sun, B.Q. Ming, P. Qi, L.M. Zheng, J. Du, C.M. Wang, S.J. Zhang, T.R. Shrout, Scripta Mater. 59 (2008) 115.
[12] C.M. Wang, J.F. Wang, Appl. Phys. Lett. 89 (2006) 202905.
[13] C.W. Ahn, I.W. Kim, M.S. Ha, W.K. Seo, J.S. Lee, S.S. Yi, Ferroelectrics 273 (2002) 2639.
[14] J.S. Kim, C.W. Ahn, D.S. Lee, I.W. Kim, J.S. Lee, B.M. Jin, S.H. Bae, Ferroelectrics 332 (2006) 45.
[15] J.J. Liu, C.X. Gao, G.T. Zou, Y.R. Jin, Phys. Lett. A 218 (1996) 94.
[16] E.V. Ramana, V.V. Kiran, T.B. Sankaram, J. Alloys Compd. 456 (2008) 271.
[17] Z.F. Li, C.L. Wang, W.L. Zhong, J.C. Li, M.L. Zhao, J. Appl. Phys. 94 (2003) 2548.
[18] A. Sanson, R.W. Whatmore, Jpn. J. Appl. Phys. 41 (2002) 7127.
[19] M.L. Zhao, C.L. Wang, W.L. Zhong, J.F. Wang, H.C. Chen, Acta Phys. 52 (2003) 229.
[20] G.O. Jones, P.A. Thomas, Acta Crystallogr. Sect. B 58 (2002) 168.